Uncertainties of Numerical Structural Models in the Frame of Aeroelasticity

P. Reich, A. Reim, M. Haupt, and P. Horst

Abstract. Today, numerical methods for structural and aerodynamic problems are reaching highly versatile and reliable levels. Therefore, the coupling of both domains can be solved at a high standard. On the other side, the accuracy of aeroelastic analyses depends on the level of precision with which the stiffness properties and, thus the structural behavior of an aircraft wing structure in means of deformation can be predicted. The presence of uncertainties within the structural model which is integrated in the coupled analysis can affect the fidelity of the structural response and, thus, influence the results of the numeric aerodynamic simulation as well. Investigations carried out by the Institute of Aircraft Design and Lightweight Structures (IFL) in the frame of the MUNA-project were focused on two types of uncertainties affecting the accuracy of the static aeroelastic analysis: stochastic uncertainties and uncertainties due to modeling simplifications. Stochastic uncertainties are caused by the deviation of actual structural parameters in realized aircraft wings, like Young's modulus or wall thicknesses from the original ideal design. This deviations affect the stiffness of the real structure and, thus the structural and aerodynamic response. A method to estimate the sensitivity of the wing structure to random input parameters is presented in the second part. The second class of uncertainties arises from approximations connected to the idealization of the physical and geometric properties of the real structure used in finite element (FE) structural models. In the first part of this work, an overview of modeling effects is given which affect the stiffness properties of the FE structural models and in turn influence the results of static aeroelastic analysis. The coupled analysis is carried out with a high-order panel method for the aerodynamic domain and a parametric finite element structural model, which allows a wide variation of material and geometric properties of wing box structure. This structural model as well as the aerodynamic method and the coupling routines are presented in the following section.

P. Reich, A. Reim, M. Haupt, and P. Horst
IFL, Hermann-Blenk-Str. 35, D-38108 Braunschweig
e-mail: paul.reich@tu-bs.de

B. Eisfeld et al. (Eds.): *Management & Minimisation of Uncert. & Errors*, NNFM 122, pp. 157–180.
DOI: 10.1007/978-3-642-36185-2_7

1 Finite Element Models and Analysis Methods Used for Uncertainty Quantification

1.1 Parametric Finite Element Model

A code already developed at the Institute of Aircraft Design and Lightweight Structures (IFL) is enhanced to generate a finite element model of the structure. It is based on the parametric description of airplane wing geometry and a layout of the load-bearing structure [1], [2]. The code is written in Patran Command Language (PCL) which allows an automated generation of finite element wing models by the preprocessor MSC Patranő.

A HIRENASD wind tunnel model [3] scaled up to 58 m of span is employed as a test structure for investigations carried out in the context of the MUNA project. The wing box structural layout and the arrangement of engines are taken on from the predecessing project [4] and resemble the wing of an AIRBUS A340 aircraft (see Fig. 1).

The geometric data are imported from an ASCII input file and are employed to generate a finite element shell model of the wing. A transonic transport aircraft design is used with the corresponding weights given in table 1 to evaluate the target lift for the calculation of aerodynamic and static inertial loads.

Due to a high number of required aeroelastic calculations, especially for the stochastic analysis presented in the second part of the work, the high order panel method HISSS is used instead of an Euler or RANS code to calculate the discrete aerodynamic nodal loads. The lack of accuracy when calculating a load distribution on the wing surface at higher Mach numbers had to be accepted so that the numeric costs could be kept reasonable. The finite-element solver NASTRAN was used to calculate the nodal displacements of the structural model.

The in-house code coupling library ifls [5] was employed to perform the fluid-structure interaction. The code handles the load and displacement transfer between non-conform grids by using a three-field approach in combination with Lagrange multipliers. The structure of the coupling routine allows the interaction between different commercial numerical solvers. The converged angle of attack α_{EqSt} of static aeroelastic equilibrium was estimated by ifls iteratively for given lift and flow conditions by variation of an overall (geometric) angle of attack α_g of the wing.

Table 1 Weights for the transonic transport aircraft design used in this study

Gross weight	m_{TOW}	to	256
Fuselage and empennage unit structure + payload	$m_{RF} + m_N$	to	95
Wing structure	m_W	to	35
Total fuel mass	m_F	to	106
Propulsion group	m_{PG}	to	20

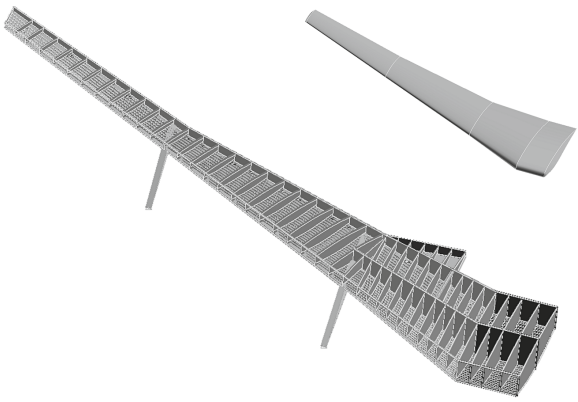

Fig. 1 HIRENASD wing geometry and structural layout

Nodal loads calculated on the aerodynamic surface were transferred to the nodes of the structural grid by means of conservative interpolation in the area of the wing box. In the region of the flap and slat structure the aerodynamic nodal loads were applied to additionally created auxiliary structural nodes and tied to the wing box by multi point constraints of RBE3 type.

The static inertial loads including fuel weight, engine loads and the weight of the flap structure had also to be taken into account to represent realistic loading conditions. The flap and slat structure were idealized as point masses and connected to the spar structure by multi point constraints in the same way as the aerodynamic forces. The masses of the high lift devices were also required for this idealization and were estimated by handbook methods [6]. Tank loads were also modeled with point masses and RBE3s. The tank masses were evaluated for each wing bay by calculation of the volume taken by the fuel for a given degree of refueling.

The static inertial loads including fuel weight, engine loads and the weight of the flap structure had also to be taken into account to generate realistic load cases. The flap and slat structure were idealized as point masses and tied to the spar structure by multi point constraints in the same way as the aerodynamic forces. The masses of the high lift devices needed for this simplified approach were estimated by handbook methods [6]. Tank loads were also modeled with point masses and RBE3s. The tank mass was estimated for each wing bay by calculation of the volume taken by the fuel for a given degree of refuelling.

The wing box structure was sized with respect to strength criteria and constraints of buckling stability. Two load cases were selected for the sizing process: a 2,5g maneuver and the landing impact (see table 1). The strength sizing was carried out by a fully stressed design using stress distribution computed for limit loads and a yield-stress criterion. The design against buckling failure was performed by handbook methods [7] using maximal allowable stresses for the compression panels

Table 2 Weights for the transonic transport aircraft design used in this study

2.5g maneuver			
Altitude	H	km	11
Mach number	Ma	-	0.82
Gross weight	m_{TOW}	to	256
landing impact			
Altitude	H	km	0
Mach number	Ma	-	0.2
Gross weight	m_{TOW}	to	182
Cruise flight (1g)			
Altitude	H	km	11
Mach number	Ma	-	0.82
Gross weight	m_{TOW}	to	256

as well as optimum design curves and semi-empirical formulas for estimation of stiffener spacing and cross-section geometry.

Due to constraints defining the highest permitted elastic deflection of the wing tip given in [4], the wing box was also sized under consideration of stiffness. For this additional sizing procedure the contribution of structural members to the wing deflection was calculated following the pattern of the modified fully utilized design method (MFUD) proposed by Patnaik et al [8]. For the constrained degree of freedom (in this case it is the bending displacement) the sensitivity factors can be calculated for each component of the structure. These factors are defined as dw/dm where dw is a partial change of displacement and dm is a change of structural mass. The change of bending deformation and structural mass are evaluated by attaching additional material (by increasing wing thickness or stiffener cross-section) to each structural member and recalculating the displacement w of the modified structure subjected to a reference load case. These sensitivity factors are used within the MFUD-procedure to weigh the increase of wall thickness of the structural members until the displacement constraint is achieved. This method permits to attach an additional structural mass only in those areas of the wing box whose stiffness influences the given deformation at most. The weight of the structure sized with this approach was estimated to be very close to those obtained by a time-consuming optimization procedure [8].

1.2 Quantification of Uncertainty

For the quantification of uncertainty affecting the static aeroelastic response different structural and aerodynamic output parameters are considered. Evaluation criteria commonly used for characterization of the aeroelastic response are the lift and drag coefficients for a given angle of attack, natural frequencies, or flutter speed of

the investigated aircraft. In this study only static aeroelasticity is treated, therefore the study is concerned with the aerodynamic performance of an aircraft wing under cruise flight conditions (see table 2). For this purpose the converged angle of attack α_{EqSt} is evaluated iteratively for a given lift. A coupled fluid structure analysis is performed using derivates of the wing structural model presented in section 1.1 which is affected by different types of uncertainties. For each derivate relative deviation $\Delta\alpha_{EqSt}/\alpha_{EqSt}$ compared to the result obtained for a reference structure (without modifications) is calculated.

The global values for relative difference to the converged angle of attack $\Delta\alpha_{EqSt}/\alpha_{EqSt}$ presented in this work are influenced not only by the change of structural parameters, but are dominated by the aerodynamic properties of the wing as well as by the given flow conditions and aerodynamic method used within the static aeroelastic analysis. For this reason, the results presented within this work should be considered as sample values to demonstrate the degree of deviation within aerodynamic output parameters for a special test case.

To examine the change within the wing box stiffness the structural response (without aeroelastic coupling) is calculated for different derivates of the FE test model subjected to a reference load case. The reference load case is represented by a pressure distribution and inertia loads obtained for a reference structure under cruise flight conditions. Local values of bending angle $w'(y)$ and twist $\Theta(y)$ are computed along the structural wing span. These "beam-like" deformations are extracted from the nodal solution of the 3D finite-element model by means of the method presented by Malcolm and Laird [9]. The procedure employs a least squares fitting to extract three translational and three rotational section deformations from the nodal displacements in x-, y- and z-direction for each wing section. This process is applied to a series of sections along the wing span to calculate the bending and torsion. For the local values of bending and torsional angle the deviations $\Delta w'(y)$ and $\Delta\Theta(y)$ are calculated relative to the deformations obtained for the reference structural model. The local deviations are related to the maximum reference values of the corresponding deformation, $w'(y)_{max}$ and $\Theta(y)_{max}$ respectively. This approach ensures that no singularities can occur due to very small local values within the torsion deformation.

To estimate the effect of stiffness variation on the wing aerodynamics, a well-known concept for the elastic angle of attack α^{el} is used. This kinematical term describes the local change of the geometric angle of attack α^{g} in flight direction due to elastic deformation of the wing. It affects the load distribution caused by the flexible structure of lifting surface and thus the overall lift coefficient. Deviations in torsion and bending stiffness of the wing box cause a change of the lift distribution over the wing span compared to the reference structure. Under conditions of steady cruise flight this lift change must be corrected by adapting the angle of attack α^{g} of the aircraft iteratively until target lift will be achieved and $\alpha_{EqSt} = \alpha^{g}$.

For swept wings the local angle $\alpha^{el}(y)$ depends on the torsion deformation $\Theta(y)$ as well as on the bending angle $w'(y)$:

$$\alpha^{el} = \Theta\cos\varphi - w'\sin\varphi \tag{1}$$

From the kinematical interrelationship in equation (1) follows that for a wing with positive angle of sweep back φ the torsion and bending contributions of the elastic angle of attack are directed mutually. For this reason, the change of bending angle due to reduction of bending and shear stiffness of the wing box structure can be compensated by the change of torsion deformation caused by the reduced torsion stiffness to a certain degree. For common transonic transport aircraft wing structures the angle α^{el} is dominated by the bending deformation and for this reason is negative.

To estimate the effect of the variation of torsion and bending distortions on the deviation of the elastic angle the propagation of uncertainty is applied on equation (1). For a local relative deviation $\Delta\alpha^{el}(y)/\alpha^{el}_{max}$ in elastic angle of attack a mathematical correlation (2) is the following:

$$\frac{\Delta\alpha^{el}(y)}{\alpha^{el}_{max}} = \frac{\Delta\Theta(y)}{\Theta_{max}}\left(\frac{\Theta_{max}}{\alpha^{el}_{max}}\right)\cos\varphi(y) - \frac{\Delta w'(y)}{w'_{max}}\left(\frac{w'_{max}}{\alpha^{el}_{max}}\right)\sin\varphi(y) \tag{2}$$

The local values $\Delta\Theta(y)/\Theta_{max}$ and $\Delta w'(y)/w'_{max}$ are relative deviations of torsion and bending distortions due to the local change of wing box stiffness caused by different degrees of modeling simplification. These values are structural parameters depending on the stiffness properties of the structure. The terms $\Theta_{max}/\alpha^{el}_{max}\cos\varphi$ and $w'_{max}/\alpha^{el}_{max}\sin\varphi$ in equation (2) are ratios of the local torsional and bending angles relative to the maximum value of elastic angle of attack. These values depend on the local sweep back angle $\varphi(y)$ of the wing box reference axis, the load distribution in chord and span-wise directions (ratio of the distributed moment relative to the distributed load) as well as on the ratio of the torsion stiffness *GJ* relative to the bending stiffness *EI*.

The local deviations of the elastic angle of attack $\Delta\alpha^{el}(y)/\alpha^{el}_{max}$ are related to the maximum value obtained for the reference FE model in the same manner like deviations of structural deformations. Since the effect of the deviation of this parameter on the geometric angle of attack α^{g} and thus on the local lift distribution is depending on the magnitude of $\alpha^{el}(y)$ this approach seems to be more suitable for the objective of the present study than relating this term to the reference local values as commonly done. The latter method would overestimate the influence of the deviation $\Delta\alpha^{el}(y)$ considering local variations of the elastic angle of attack near the root as well, which have no appreciable effect on the load distribution due to the very small values of $\alpha^{el}(y)$ within this area.

The distribution of the local deviations $\Delta\Theta(y)/\Theta_{max}$, $\Delta w'(y)/w'_{max}$ and $\Delta\alpha^{el}(y)/\alpha^{el}_{max}$ varies along the wing structural axis, depending on the stiffness and load distribution of the present wing structure and aerodynamic design. To obtain global deviation parameters the mean values of these local variations are calculated in sections using a relation defined exemplary in equation (3) for the bending angle:

$$[\Delta w'] = \frac{1}{s}\int_0^s \frac{\Delta w'(y)}{w'_{max}}\,dy \tag{3}$$

where s is the structural span of the wing box. Mean values of twist $[\Delta\Theta]$ and elastic angle of attack $[\Delta\alpha^{el}]$ are obtained in the same way. To assess the contribution of the variations of torsional and bending angles to the deviation of elastic angle of attack, the local values $\Delta w'(y)/w'_{max}$ and $\Delta\Theta(y)/\Theta_{max}$, multiplied with the parameters' terms $w'_{max}/\alpha^{el}_{max}\sin\varphi$ and $\Theta_{max}/\alpha^{el}_{max}\cos\varphi$ from equation (2), are integrated by means of eq.(3). These "transformed" values $[\Delta w']_{tr}$ and $[\Delta\Theta]_{tr}$ are also used within the present work to estimate the effect of variation within structural stiffness properties caused by modeling or stochastic uncertainties on the load distribution. The difference between the term $[\Delta\alpha^{el}] = [\Delta\Theta]_{tr} - [\Delta w']_{tr}$ calculated from the global bending and torsion deformations and the mean value resulting from integration of the local values $\Delta\alpha^{el}(y)/\alpha^{el}_{max}$ directly obtained from the structural response is between 0.01% and 0.03%.

Because nonlinear behavior of aeroelastic problems is highly depending on the local flow conditions as well as on local stiffness characteristics of the wing structure, the change in equilibrium state angle of attack $\Delta\alpha_{EqSt}/\alpha_{EqSt}$ cannot be predicted using a mean value $[\Delta\alpha^{el}]$ for a complex structure in a direct way. Nevertheless, as will be shown within the following sections, the parameter $[\Delta\alpha^{el}]$ is a suitable indicator to estimate the deviation tendency of wing aerodynamics due to the variation within the stiffness properties of the wing.

2 Part I: Model Uncertainties

2.1 Introduction

To obtain a high level of accuracy for a structural model one possible approach is to reproduce the real structure with a high level of geometric detail. This approach implies two general drawbacks: it is connected with high modeling effort on the one hand and requires fine discretization of the wing box geometry on the other hand (see Fig. 4, on the left hand side), resulting in high model size and numerical costs. To demonstrate the dimension of complexity connected with a detailed model the reference structure described in section 1.1 is considered. The FE model has 740 design variables and is realized by 24900 shell and 10700 bar elements having in total 260000 degrees of freedom.

For coupled aeroelastic analysis, requiring a high number of iterations the minimization of the finite element model size could be of high priority. As first approach to reduce the number of degrees of freedom, reduction techniques are used to condense a 3D wing box structural model into a 1D-beam stick model. In the other case, if a parametric FE wing model with variable geometry should be optimized, the amount of design variables associated with high level of modeling detail is undesirable. To reduce the number of design variables a simplified structural model is preferred which is composed only of main components of the wing structure, like top and bottom covers, ribs and spars, including spar caps. Within such

simplified models stringer stiffeners are commonly idealized by an additional layer with orthotropic material properties. The next sections deal with the effect of the simplifications within the 3D FE models.

2.2 Design of the Wing Structure

The structure of a common transport aircraft wing is composed of the following components (see fig. 2):

- Spars with spar webs carrying shear load and spar caps which resist tension or compression normal loads. Generally, the wing box is composed of a front and rear spar. The rear spar is of special importance for the mounting of movables as well as for systems integration. As shown in fig. 2, additive components, like a mid-spar, or a false rear spar can be integrated in the wing structure as well.
- Top and bottom covers which have a contouring as well as a load carrying function. These components carry both, normal and shear stresses. Along with main spars, the wing skin forms the box structure of the wing. The skin parts are stiffened by stringers to prevent buckling failure
- Ribs which can be oriented perpendicular to the wing box axis or parallel to the aircraft symmetry plane. Ribs are used to keep the aerodynamic shape of the wing cross-sections under aerodynamic load and for insertion of concentrated loads in the wing box structure caused by engine mountings or landing gear.

In figure 2 different levels of modeling details for each structural component are depicted. The stiffening components, like stringers, spar- or rib caps can be realized by beam elements with defined cross-sections, by rod elements neglecting the bending stiffness of the stiffener or can be "smeared" over the area of the correspondent thin-walled structural component. The smeared stiffening component in turn can be realized as an additional orthotropic material layer, which is reasonable when modeling the skin-stringer panels or taken into account in the wall thickness of the thin-walled components what is commonly done by ribs and spars.

In the current study the structural model is realized by shell and bar elements. The inclusion of element offsets was used as a reference with highest grade of modeling detail limited to the main stiffening components within the present work.

The different levels of detail, shown in figure 2 are employed within the test wing model. The idealized FE models are derived from the reference geometry by replacing the built-up structure, realized with shell and bar elements, by a.m. simplified structural design. To estimate the deviations in the deformation behavior caused by modeling simplifications the structural response of both the reference and simplified wing box models is compared for a reference loading. To ensure the comparability of these results the volume of the wing structure was kept constant for all derivations with varying grade of the detail.

Uncertainties caused by different levels of approximation are discussed in the following section. The intent of this overview is not to enable the general prediction

of the modeling error of the structural and thus of the aeroelastic response resulting from distinct simplification. Due to the individual design and stiffness properties of wing structures realized in different aircraft types the contribution of structural components to the bending, shear, and torsional stiffness as well as to the warping characteristics varies depending on a given structural design. Instead of that, a series of calculations is performed to estimate the dimension of the deviations resulting from different levels of simplification using the parametric finite element model. The effect of uncertainty on the stiffness properties of the wing structure is considered only in the frame of static aeroelastic analysis under assumption of linear elastic structural behavior. Non-linear effects as well as dynamic properties or effects caused by the usage of non-isotropic materials are not in the objective of the present work.

2.3 Uncertainties due to Modeling Simplifications

A series of comparing analyses is carried out to estimate the influence of geometrical details on the accuracy of wing structural response. Global deviation parameters presented in section 1.2 are used to evaluate at first the change in structural stiffness components due to modeling approximations and secondly the influence of these alterations on the static deformation of the wing in flight direction considering the elastic angle of attack α^{el}. For selected cases a static aeroelastic analysis is carried out to calculate the deviation of equilibrium state angle of attack and, therefore, to estimate the impact of altered structural stiffness on the aeroelastic response. To

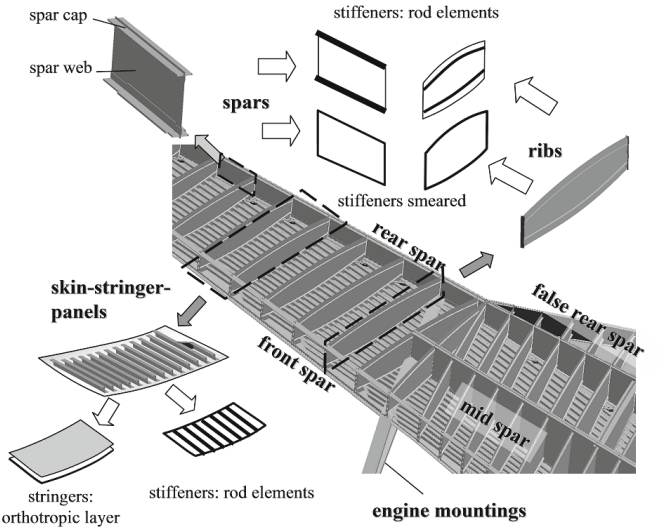

Fig. 2 Components of the wing box structure

distinguish the deviations of structural stiffness five integral parameters are listed in tables 3 and 4 for each modeling effect. These parameters are the integral deviation of bending and torsional angles $[\Delta w']$ and $[\Delta\Theta]$ relative to the elastic axis of the wing, the "transformed" values $[\Delta w']_{tr}$ and $[\Delta\Theta]_{tr}$ of both angles in flight direction as well as the global deviation of elastic angle of attack, $[\Delta\alpha^{el}]$.

2.3.1 General Simplifications

Effect of the Element Offset

To reproduce the outer mold surface of the real wing structure the shell elements forming the wing skin must have an offset relative to the nodes of the discretized geometry. By neglecting the element offset the distance of skin panels relative to the neutral axis of the wing box will be overestimated. This effect will increase the moment of inertia of the wing box cross-section following the parallel axis theorem, which in turn results in higher bending stiffness of the wing structure compared to the exact solution. The torsional stiffness will also be affected by the increasing distance between the mid-lines of the top and bottom covers in accordance with the Bredt-Batho formulation. The same effect on the bending stiffness appears by ignoring the offset distance of beam or rod elements representing the stiffening structural members. The latter case will be considered separately for each stiffening component.

To estimate the impact of the modeling simplifications on the deformation behavior of the wing box the structural response is calculated for the idealized and the reference structural models. The integral values of the deviation in bending angle, torsion and resulting elastic angle of attack compared to the reference structure are given in table 3. For the FE wing model without element offset within the top and bottom covers the bending stiffness increases accordingly to the a.m. effects resulting in an approximately 4% smaller bending angle which in turn reduces the local angle of attack (cp. section 1.2). Torsion deformation is also reduced by 1.7% due to the higher torsional stiffness having an opposite effect. The change in both degrees of freedom results in 4.1% smaller elastic angle of attack due to the dominant influence of the bending stiffness (compare the values $[\Delta w']_{tr}$ and $[\Delta\Theta]_{tr}$ in table 3). The sign of the transformed deviation parameter $[\Delta\Theta]_{tr}$ changes due to the relation to the maximum value of elastic angle of attack α^{el}_{max}.

The converged angle of attack calculated for the more simplified structure shows a 0.9% smaller value compared to the reference model (see fig. 5). This result corresponds with the trend predicted by the negative change of the elastic angle of attack $[\Delta\alpha^{el}]$ given in table 3. Smaller (negative) values of $\alpha^{el}(y)$ along the span have a reduced effect on the load distribution compared to the reference structure and, therefore, the target lift can be achieved under smaller angle of attack.

Table 3 Deviations of bending angle, torsional angle and elastic angle of attack for different states of modeling simplification

	shell elems. without offset		simplified BCs	
	rel. glob. deviation	rel. glob. deviation: transf.	rel. glob. deviation	rel. glob. deviation: transf.
$[\Delta w']/[\Delta w']_{tr}/\%$	-3.955	**-4.327**	-5.446	**-5.782**
$[\Delta\Theta]/[\Delta\Theta]_{tr}/\%$	-1.699	**0.228**	-29.534	**3.974**
$[\Delta\alpha^{el}]/\%$		**-4.101**		**-1.806**

Simplified Boundary Conditions

At the root, the wing is mounted to the wing center box and to the main frames of the fuselage. Despite of high local wing box stiffness, a minimal translational displacement of the wing skin in span wise direction is possible in the root area. If this infinitesimal displacement is constrained by restriction of all translational and rotational degrees of freedom along a root rib curve (see fig. 3, on the right hand side), a reduction of bending and torsion deformations due to the overestimation of wing root rigidity can appear. This kind of idealization is used when the structure of a half wing is realized without the center box. To assure realistic boundary conditions, see figure 3 on the left hand side, the displacement of upper and lower edges of the root rib, should be constrained only in direction normal to the skin surface (z-direction). The nodal displacements in spanwise direction (along the y-axis) as well as nodal rotations have to be constrained only at the symmetry plane of wing center box.

The effect of higher wing root rigidity has a local character influencing the bending and torsional deformations in the form of additional (negative) rigid body motions, resulting in the integral deviation of 5.4% within the bending and approx.

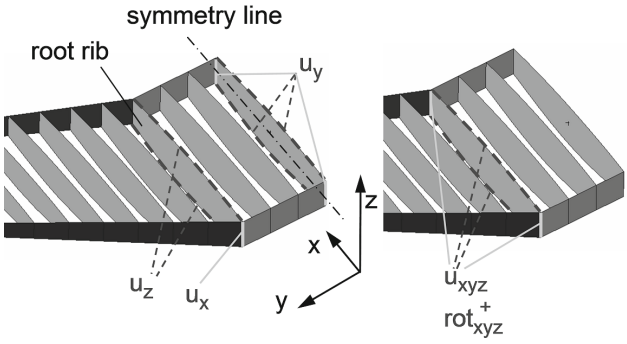

Fig. 3 Realistic and simplified boundary conditions

30% within the torsional angle. Due to the mutually directed influencing tendencies of these deformations, the resulting change within the elastic angle of attack is only 1.8% (see table 3). From the transformed values $[\Delta w']_{tr}$ and $[\Delta\Theta]_{tr}$ in table 3 it can be seen that the rather high contribution of bending deviation in flight direction is compensated by the much higher change of the torsional angle.

The results of the coupled aeroelastic analysis confirms with the tendency of the deviation of elastic angle of attack $\alpha^{el}(y)$ obtained by the structural response. This moderate tendency of the change of is reflected in the deviation of the equilibrium state angle of attack $\Delta\alpha_{EqSt}/\alpha_{EqSt}$ being only 0.54% (see fig. 5).

2.3.2 Idealization of Stiffened Structural Components

In the following sections, the effects of the different degrees of detail of modeling are discussed. Several types of stiffener idealization are considered and the effect of the simplifications on the structural behavior and aerodynamic properties of the wing is evaluated by calculating structural and static aeroelastic response. The deviations of structural response computed for each case are summarized in a test matrix (see fig. 4). In the test matrix, different degrees of modeling detail are considered for stringers, spar caps and rib caps. The levels of modeling detail are represented by realizing the structural member by beam elements or rod elements, or by homogenizing the stiffeners as isotropic or orthotropic layer. The effect of element offset is also considered for beam and rod elements as well as for the orthotropic material layer. For the main idealizations, the deviation of converged angle of attack from the reference case is plotted in figure 6.

		stringers		spar caps		rib caps	
		rel. glob. deviation	rel. glob. deviation: transf.	rel. glob. deviation	rel. glob. deviation: transf.	rel. glob. deviation	rel. glob. deviation: transf.
bar elems. w-out offset	**[Δw'] / [Δw']$_{tr}$** /%	-5.787	**-6.442**	-0.548	**-0.601**	-0.0131	**-0.0149**
	[Δθ] / [Δθ]$_{tr}$ /%	-0.224	**0.032**	-0.455	**0.061**	0.0172	**-0.0029**
	[Δa^{el}] /%		**-6.409**		**-0.540**		**-0.0178**
rod elems. + offset	**[Δw'] / [Δw']$_{tr}$** /%	0.843	**0.940**	-0.041	**-0.044**	0.0375	**0.0408**
	[Δθ] / [Δθ]$_{tr}$ /%	0.476	**-0.073**	-0.402	**0.055**	-0.0896	**0.0140**
	[Δa^{el}] /%		**0.866**		**0.010**		**0.0547**
rod elems. w-out offset	**[Δw'] / [Δw']$_{tr}$** /%	-5.289	**-5.889**	-0.513	**-0.563**	0.0331	**0.0351**
	[Δθ] / [Δθ]$_{tr}$ /%	0.603	**-0.096**	-0.777	**0.105**	-0.1439	**0.0222**
	[Δa^{el}] /%		**-5.984**		**-0.457**		**0.0573**
add. othotr. layer w.-out offset	**[Δw'] / [Δw']$_{tr}$** /%	-3.851	**-4.288**				
	[Δθ] / [Δθ]$_{tr}$ /%	-1.137	**0.169**	-		-	
	[Δa^{el}] /%		**-4.119**				
add. othotrop. layer + offset	**[Δw'] / [Δw']$_{tr}$** /%	0.647	**0.724**				
	[Δθ] / [Δθ]$_{tr}$ /%	-0.086	**0.011**	-		-	
	[Δa^{el}] /%		**0.735**				
add. isotrop. layer + offset	**[Δw'] / [Δw']$_{tr}$** /%	-3.944	**-4.383**	-0.986	**-1.075**	0.0039	**0.0042**
	[Δθ] / [Δθ]$_{tr}$ /%	-6.261	**0.963**	-1.968	**0.267**	0.7831	**-0.1218**
	[Δa^{el}] /%		**-3.419**		**-0.807**		**-0.1176**

Fig. 4 Deviations of structural deformations obtained for different levels of simplified stiffener modeling

Effects of Simplified Stringer Modeling

Explicit modeling of stringer stiffened top and bottom covers including property association for stiffening members is very time-consuming especially if the stringer cross-section geometry varies in both chord and span wise directions. Several degrees of stringer idealization are considered within the present study. A common method to avoid the modeling effort is to create a skin-stringer-"laminate" with isotropic skin and orthotropic stringer layers. The benefit of this approach is that only one parameter is required to realize the skin-stringer-structure. This parameter is the area ratio of the skin and summarized stringer cross-sections, commonly given in the literature as 100:50 for thee design of transport aircraft wing structures [7]. The structural model with stringers smeared as an isotropic layer presents the simplest approach concerned in the present study.

Homogenizing discrete stringers over the skin area has two opposite effects on the bending stiffness of the wing box. The first effect is the reduction of the wing box local moment of inertia by neglecting the bending stiffness of the stringers. The second effect is the overestimation of the wing bending stiffness caused by neglecting the (offset) distance of the stringer cross-sections relative to the skin surface. The effect of ignoring the bending stiffness of the stiffeners on the bending and torsional deformation of the wing can be concerned on the basis of deviations obtained for a FE model with stringers realized with rod elements. For this idealization, the bending angle is increased by only 0.84% due to lower structural stiffness, resulting in 0.87% greater angle of attack. The influence of stringer stiffness on the torsional behavior and in turn on the elastic angle of attack is negligible (see table 4). The marginal impact of stringer bending stiffness on the deformation behavior results in change of geometric angle of attack being only 0.19% (see fig. 6).

In contrast to the effect of the stringer-stiffness, the overestimated contribution of the stringer-cross-sections to the local wing box moments of inertia due to non-considering the correct offset distance dominates the influence on the bending deformation. How can be seen in table 4 for the deviations obtained for FE models with stringers idealized as isotropic and orthotropic layer without offset, the bending angle decreases by $3.9 - 4\%$. Because stringers do not contribute to the shear load resistance of skin panels the stringer idealization as an orthotropic material layer enables to reproduce the torsional stiffness of the wing box structure in the way that

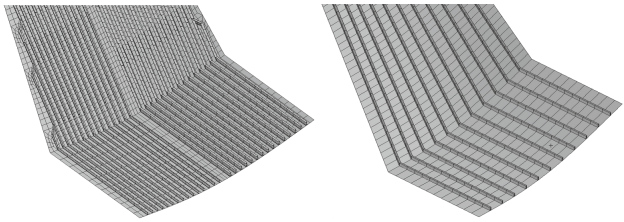

Fig. 5 Different levels of stringer modeling detail

is more realistic compared with stringers homogenized as isotropic material. This trend is demonstrated by the smaller deviation of twist ($[\Delta\Theta] = 1.1\%$) compared to the simplest model ($[\Delta\Theta] = 6.3\%$). One remarkable effect of greater difference of wing twist is the smaller deviation of elastic angle of attack of the structural model with stringers idealized as isotropic layer ($[\Delta\alpha^{el}]$ = -3.4%) compared with the more realistic approach ($[\Delta\alpha^{el}] = -4.1\%$). The trend predicted by the comparison of the $[\Delta\alpha^{el}]$-deviation parameters between the both structural models, confirms with the results of static aeroelastic analysis. The deviation of converged angle of attack for the skin-stringer compound realized with orthotropic stringer layer is slightly higher ($\Delta\alpha_{EqSt}/\alpha_{EqSt} = -0.82\%$) as for a simpler structure ($\Delta\alpha_{EqSt}/\alpha_{EqSt} = -0.71\%$, see fig. 6).

Effect of Simplified Spar Cap and Rib Cap Modeling

Effects occurs by modeling the spar caps with beam or rod elements with or without considering element offsets are similar to those discussed in the section above. Due to smaller cross-section of the spar caps relative to the cross-section of the whole wing box this effects causes only marginal discrepancies of the bending and torsion angle and thus of the elastic angle of attack. If spar stiffeners are considered as isotropic layer in the wall thickness of the skin parts the bending stiffness increases causing 0.8% smaller elastic angle of attack. The deviation $[\Delta\alpha^{el}]$ that results from neglecting the element offsets varies between -0.46% and -0.54% (see fig. 4). A static aeroelastic response was calculated for wing structure with spar caps modeled with bar elements without element offset. The converged angle of attack

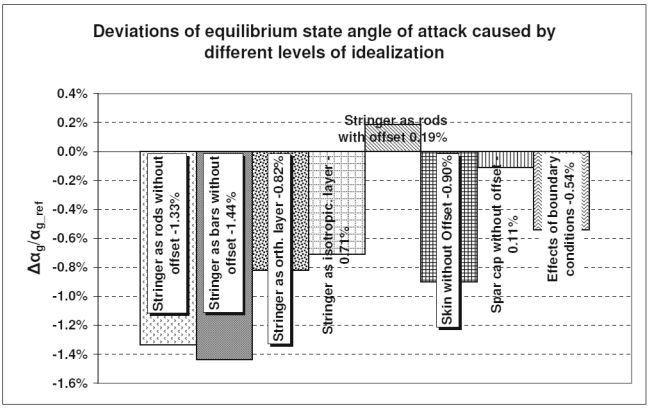

Fig. 6 Deviations of equilibrium state angle of attack for different variants of modeling simplification

α_{EqSt} of this structure is only 0.11% smaller compared to the reference structure. How can be seen from results in table 4 the influence of rib caps on the bending and torsional deformation is marginal resulting in deviations of elastic angle of attack being between 0.02% and 0.2%. Therefore, the influence of these stiffening components on the deformation behavior and thus on the aerodynamics of the wing can be neglected.

2.3.3 Conclusions

Within the first part of the work, a simple method was presented to calculate global parameters, which enables to estimate the effect of uncertainties of structural models on the deformation behavior and thus on the aerodynamic properties of the wing structure. This method was applied to investigate the impact of modeling uncertainty on the structural and aeroelastic response of the wing of a wide-body transport aircraft. The results of the study yield a rather good agreement between the deviation trends of the structure subjected to modeling uncertainty, which are calculated for a static loading and the discrepancy of aerodynamic properties of the wing obtained by a coupled analysis. As mentioned above, the elastic angle of attack α^{el}, employed as evaluation parameter is dominated by the bending deformation of the wing structure. Since the top and bottom covers have the greatest contribution to the bending stiffness of the wing, the simplified modeling of stringers has the major effect on the accuracy of the structural model. The deviations of converged angle of attack α_{EqSt}, used as performance criterion to evaluate the accuracy of the coupled analysis varies between 0.2% and 1.44% for different degrees of modeling detail (see fig. 6).

As shown on the sample of simplified boundary conditions, the higher deviations of twist and bending angle must not as well produce higher discrepancy of converged angle of attack. In fact the deviations has to be transformed in flight direction using the interrelationship give in equation (2) to estimate the resulting effect of the discrepancies within both deformations on the load distribution.

3 Part II: Stochastic Simulations

3.1 Introduction

In the second part, the effects of stochastic uncertainties on the accuracy of static aeroelastic analysis are investigated. A parametric finite element model (see section 1.1) is used to simulate the scatter of the structural input parameters expressed as Gaussian standard normal distribution. Coupled aeroelastic analysis is performed to obtain the deviation of the wing aerodynamics for a discrete distribution of the stochastic input parameters using a high order panel code. A first order reliability method is employed to calculate the probability of change of aerodynamic performance parameters due to the variation of structural stiffness properties. The

results of the stochastic analyses performed for a simple test case are presented and demonstrate robust behavior of a coupled aeroelastic system subjected by moderately arbitrary structural parameters.

3.2 First Order Reliability Method

In the present work, the probability of failure P_f of the wing structure is computed. It describes the probability that the structure does not to comply with the predefined requirements. Thus, the term failure has to be distinguished from other terms, like e.g. crash or disaster. Since the coupled fluid-structure analyses are very time consuming, the first order reliability method (FORM) was implemented to calculate the stochastic characteristics of the wing [10]. FORM introduces the reliability index β to describe the reliability of the structure. The main input to the method is the limit state function $G(\mathbf{X})$, where $\mathbf{X}$ is the vector of stochastic variables that influence the structure. By definition, the limit state function is positive, if the structure fulfils its requirements. Negative values are returned, if at least one requirement is violated.

In order to generate unique results for every problem, the vector of stochastic variables is transformed into a vector of standard normal random variables $\mathbf{X}$. This leads to a limit state function $G(\mathbf{X}')$ which is analyzed using the FORM routine. The FORM is a gradient based optimization procedure which calculates the minimum distance β between the limit state function defined by $G(\mathbf{X}') = \mathbf{0}$ and the origin of the standard normal variable space spanned by the normalized stochastic variables.

At the beginning of the FORM algorithm, a $\beta_{initial}$ has to be estimated. The better the estimation of this initial value factor the fewer iterations are needed in the algorithm to get the final β. With the $\beta_{initial}$ and the limit state function value, all parameters are defined to start the main iteration of the FORM algorithm consisting of three main steps: (cp. Haldar, Mahadevan [11])

- Transformation of stochastic variables into standard normal variable space. In order to get unique results, all non-standard normal variables have to be transformed. For normal variables, a general conversion can be applied, for other variables, the Method of Rackwitz and Fiessler [12] has to be used.
- Generation of derivatives of the limit state function with respect to the standard normal variables. The coupled fluid-structure model can not be solved algebraically. Thus, the derivatives have to be estimated by finite differences in the neighbourhood of the design point.
- Calculation of the direction, where the steepest trend in the limit state function occurs and estimation of a new design point and the corresponding β value

This iteration is repeated until the limit state function value is zero and the β value converges. The resulting β value is then transferred to the fitness value calculation routine of the optimization.

3.3 Combination of the FORM-Routine with Fluid-Structure Interaction Code Library

To simulate an impact of variation of structural parameters on the aeroelastic response of the wing, the ifls-code-library was embedded into the routines performing the FORM algorithm. A NASTRAN input file of the finite element wing model was created with the ability to vary the structural properties during the stochastic process. Two input parameters are defined to be altered within the wing box structure: the thickness t of the thin-walled structural members and the Young's modulus E of the material. For stochastic input parameters a normal distribution is assumed. The shape of the normal distribution and, therefore, the extent of the deviation of the input parameters are characterized by the coefficient of variation (COV) $V = \sigma/\mu$. The COV is defined as a ratio of the standard deviation σ to the mean value μ. For a random variable with $V = 0.1$ the probability is 31.7% that the deviation of this variable exceeds $\pm 10\%$.

3.3.1 Definition of the Limit State Function

To apply the FORM analysis to the coupled fluid-structure problem a realistic failure criterion had to be defined to describe the performance of the simulated wing structure. For this kind of problem the random input is given by a variation of structural parameters. The change of the converged angle of attack α_{EqSt} of the aeroelastic equilibrium state (cp. section 1.2) was used to estimate the impact of random input parameters on the aerodynamic properties of the investigated wing model. The deviation $\Delta\alpha_{EqSt}/\alpha_{EqSt}$ can be considered in both positive and negative directions. The higher values of α_{EqSt} caused by a lower Young's modulus or by reduction in wall thickness, respectively, are assessed to be more critical than smaller ones, caused by a stiffer wing structure.

The probability of deviation of equilibrium state angle of attack is investigated for different values of $\Delta\alpha_{EqSt}/\alpha_{EqSt}$ varying between 0.4% and 1.0%. Each value corresponds to a limit state function in the normal variable space, which is defined as:

$$G(\mathbf{X}') = \Delta\alpha_{EqSt} - \Delta\alpha_{EqSt,req} \tag{4}$$

The term $\Delta\alpha_{EqSt,req}$ defines the highest permitted deviation of the converged angle of attack. For a discrete limit state function and a distribution of random parameters (characterized by the coefficient of variance) the FORM algorithm calculates a combination of these parameters for which the reliability index β becomes minimum. For the inversion of the argument, the probability of the aeroelastic response represented by the limit state function becomes maximal.

An exemplary problem for two random variables X_1' and X_1' with two limit state functions $G_1(\mathbf{X}'))$ and $G_2(\mathbf{X}')$ is depicted in fig. 7. Corresponding to the definition of the reliability index β the probability of $G_1(\mathbf{X}')$ is higher then of $G_2(\mathbf{X}')$ because

of the smaller distance β between the curve and the origin of the standard normal space.

3.4 Sensitivity Analysis by a Global Variation in Structural Parameters

The variation of the wall thickness and Young's modulus causes a deviation of stiffness qualities of the wing structure. Due to manipulation of structural properties the tendency of the wing is affected to exceed its shape under a certain load. The objective of the parameter study was to estimate the impact of parameter variation within the main structural components on the structural behavior as well as on the static aeroelastic response.

The alteration of structural parameters of skin, spars, or ribs influences the torsion and bending distortions in different ways. Reduction of the wall thickness as well as of the Young's modulus in the skin parts has the highest effect on the bending and shear stiffness of the wing reducing the bending moment of inertia and shear coefficient of a local wing box cross-section. The torsional stiffness is also affected, depending on the ratio of wing box height to depth and thickness ratio of the skin to spar webs. Reduction of structural parameters in the spar webs influences mainly the torsional and shear stiffness having only a secondary effect on the bending moment of inertia. Due to the low contribution of the ribs to the bending and torsional

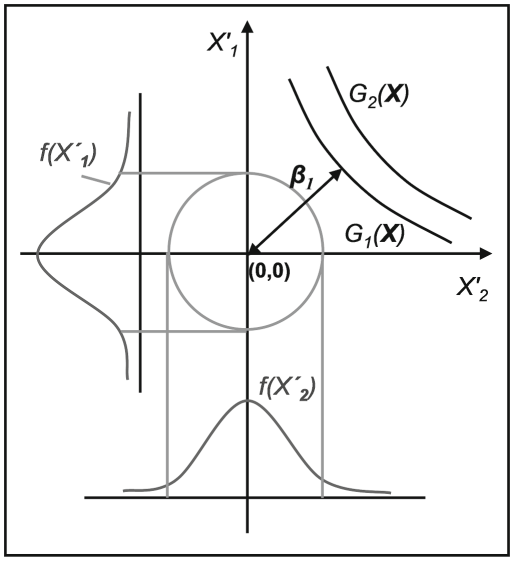

Fig. 7 Random input parameter distribution and limit state functions in the normal variable space

stiffness of the wing box structure the variation of the input parameters in this structural member has only a marginal effect on the deformation behavior of the wing.

A parameter study is carried out to estimate the sensitivity of the structural and thus of the static aeroelastic response relative to the components of the wing structure affected by uncertain input parameters. The influence of each component is estimated by changing successively the wall thickness and Young's modulus of the skin, spar webs and ribs. To avoid local effects both input parameters are varied simultaneously by $\pm 10\%$ along the wing span. A structural and an aeroelastic response of a modified structure are determined for a reference loading corresponding to the 1g load case. From the structural response, the global deviations $[\Delta\Theta]$, $[\Delta w']$ and $[\Delta\alpha^{el}]$ of torsion deformation, bending angle and elastic angle of attack including the components $[\Delta\Theta_{tr}]$ and $[\Delta w'_{tr}]$ are calculated. An alteration $\Delta\alpha_{EqSt}/\alpha_{EqSt}$ of the converged angle of attack is obtained from the results of coupled analysis by comparison with the reference structure. The results for the global deviations are given in tables 4 and 5.

The wing box investigated in the parameter study which structural properties are varied separately and in the same manner does not represent a real wing. An actual wing structure is assembled of many different parts of which the dimensions and material properties vary independently from each other. The intent of this simple

Table 4 Deviations of bending angle, twist and elastic angle of attack caused by reduction of skin thickness by 10%

	skin		spars		ribs	
	rel. glob. deviation	rel. glob. deviation: transf.	rel. glob. deviation	rel. glob. deviation: transf.	rel. glob. deviation	rel. glob. deviation: transf.
$[\Delta w']/[\Delta w']_{tr}/\%$	5.720	**6.585**	0.249	**0.280**	0.066	**0.077**
$[\Delta\Theta]/[\Delta\Theta]_{tr}/\%$	5.735	**-1.172**	-0.473	**0.098**	-0.306	**0.063**
$[\Delta\alpha^{el}]/\%$		**5.412**		**0.377**		**0.140**

Table 5 Deviations of bending angle, twist and elastic angle of attack caused by reduction of Young's modulus by 10%

	skin		spars		ribs	
	rel. glob. deviation	rel. glob. deviation: transf.	rel. glob. deviation	rel. glob. deviation: transf.	rel. glob. deviation	rel. glob. deviation: transf.
$[\Delta w']/[\Delta w']_{tr}/\%$	5.745	**6.621**	0.447	**0.508**	0.062	**0.070**
$[\Delta\Theta]/[\Delta\Theta]_{tr}/\%$	5.568	**-1.138**	-0.234	**0.049**	-0.279	**0.058**
$[\Delta\alpha^{el}]/\%$		**5.483**		**0.556**		**0.128**

approach is only to estimate the main trend of the deviation of the output parameters depending on the component of the structure in which the variation of input parameter occurs.

To estimate the tendency of change of the equilibrium state angle of attack α_{EqSt} caused by the input variation of structural components a static aeroelastic response is calculated for each modified structural model already described. The relative deviation of this angle is plotted in fig. 8 for each model derivate. The results show a good agreement with the tendencies obtained from the simple deformation study (see tables 4 and 5). The contribution of deviation of both deformation components to $\Delta\alpha_{EqSt}/\alpha_{EqSt}$ is somehow different for the variation of structural parameters in spar webs and rib surfaces. The change of the torsion angle is negative with respect to the sign convention showing therefore a stiffer torsional behavior. This tendency is due to the skewed root rib of a swept wing which influences the warping moment of inertia and, thus, the torsional behavior of the wing box.

A variation of the structural parameters shows the highest effect on the structure's stiffness and therewith on the change of the angle of attack in the skin areas as expected. The results of the structural response show that, in spite of a rather high ratio of the torsion angle to the elastic angle of attack, the latter is still dominated by the angle of bending deformation. The almost identical values obtained for $\Delta\alpha_{EqSt}/\alpha_{EqSt}$ by variation of both parameters of the skin parts should be treated as a special case taking into account the global character of the applied variations.

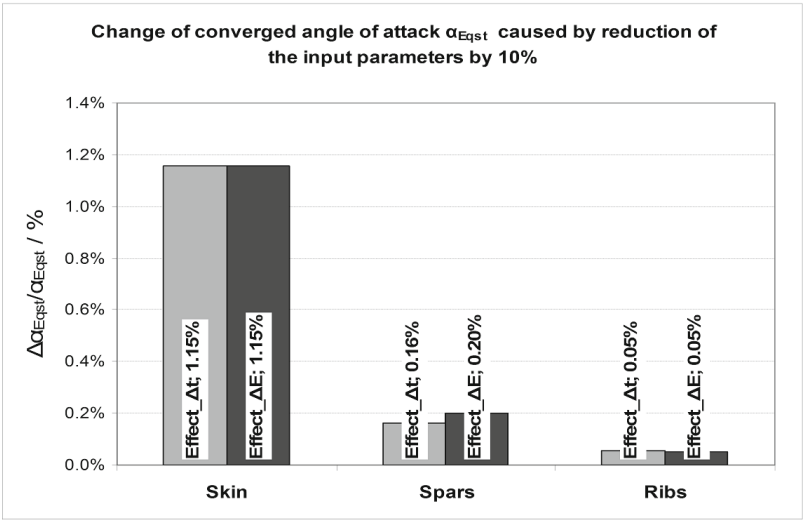

Fig. 8 Random input parameter distribution and limit state functions in the normal variable space

3.5 Results of the FORM Analysis

Within the stochastic analysis, the impact of random input parameters on the static aeroelastic response of the transport aircraft wing is investigated. Based on the results of the sensitivity analysis the analysis is performed at first only for skin areas due to the crucial impact on the wing aerodynamics. The wing structure is divided into four areas in which the input parameters were independently varied. The division of the areas is given in table 6 as a function of the span co-ordinate.

In each area, the structural parameters were varied simultaneously in the top and bottom skin parts. By this simplification, the number of random variables $\mathbf{X}_\mathbf{i}'$ decreased to a total of four that in turn led to significant reduction of numerical expenditure.

The Gaussian normal distribution for random input parameters is assumed (see section 3.2). To estimate the coefficient of variance for the thickness distribution manufacturing data sheets for maximum thickness deviation were analyzed. Following this analysis, a coefficient of variance, which lies between 0.02 and 0.04, seems to be realistic, but the results were calculated until the COV = 0.05 showed the effect of greater scatter within the input parameters. For the variation of the Young's modulus, the same coefficients are used to guarantee the comparability of the results.

The allowed relative deviation $\Delta\alpha_{EqSt}/\alpha_{EqSt}$ of the converged angle of attack compared to the reference structure is analyzed in the range between 0.4% and 1.0% for different coefficients of variation. Each value of this deviation defines a limit state function $G(\mathbf{X}')$. For a given value of $G(\mathbf{X}')$ the FORM routine calculates a combination of random variables for which the reliability index converges. With regard to the investigated problem a combination of relative deviations of the structural input parameters in each area was found for which the probability of a given deviation of the angle of attack becomes a maximum.

The results of the variation in the wall thickness and the Young's modulus in skin areas are presented in figures 9 and 10. In the diagrams a probability of failure is plotted for a series of limit state functions over the coefficient of variance V. Due to almost linear correlation between the reliability index and limit state functions for a given COV, some curves could be extrapolated from the calculated results. These curves are plotted by dashed lines. For each limit state function the probability of the failure arises with the scatter in the input parameter expressed by V. The lower

Table 6 Areas of parameter variation

Area	η_i	η_0
1	0.0	0.22
2	0.22	0.44
3	0.44	0.72
4	0.72	1.0

the allowed difference of the angle of attack expressed by a failure function is the higher is the probability to violate the requirements.

In the diagrams a probability of failure is plotted for a series of limit state functions over the coefficient of variance V. Due to almost linear correlation between the reliability index and limit state functions for a given V, some curves could be extrapolated from the calculated results. These curves are plotted by dashed lines in fig. 5 and 6. For the investigated coefficients of variance the results for a relative deviation of an angle of attack of 1.5% were calculated for the local variation in the skin thickness of 10% and more. This degree of variation within the wing structure seems not very realistic to be considered further. For each limit state function the probability of the failure arises with the scatter in the input parameter expressed by V. The lower the allowed difference in the angle of attack, expressed by a failure function the higher is the probability to violate the requirements.

The comparison of the results for variation of skin thicknesses and Young's modulus shows very similar probability curves for both input parameters. The probability of failure obtained for the variation of Young's modulus is somewhat smaller as for a variation of skin thicknesses. This tendency shows a good agreement with the predictions made within the sensibility study carried out in section 3.4.

From the results of the stochastic analysis depicted in figures 9 and 10 it can be seen that the probability of higher deviations (<1%) of the global aerodynamic properties of the wing still are very small even for a higher variance of structural parameters. This demonstrates a high robustness of the coupled fluid structure system affected by the considered type of uncertainty.

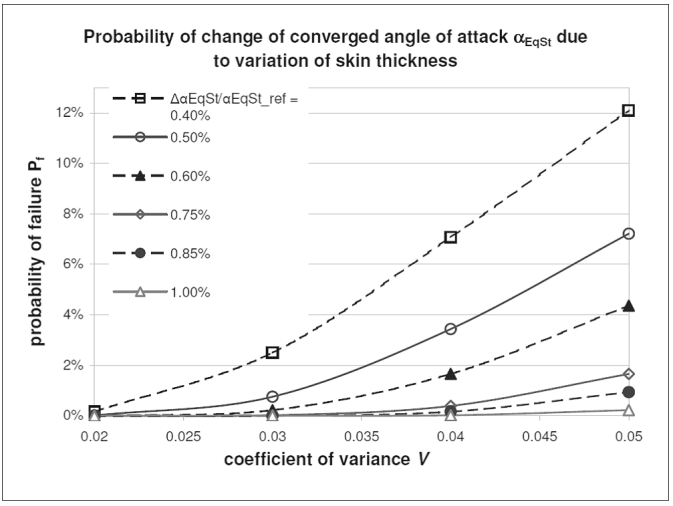

Fig. 9 Probability of deviation of angle of attack caused by variation of skin thickness for different performance criteria

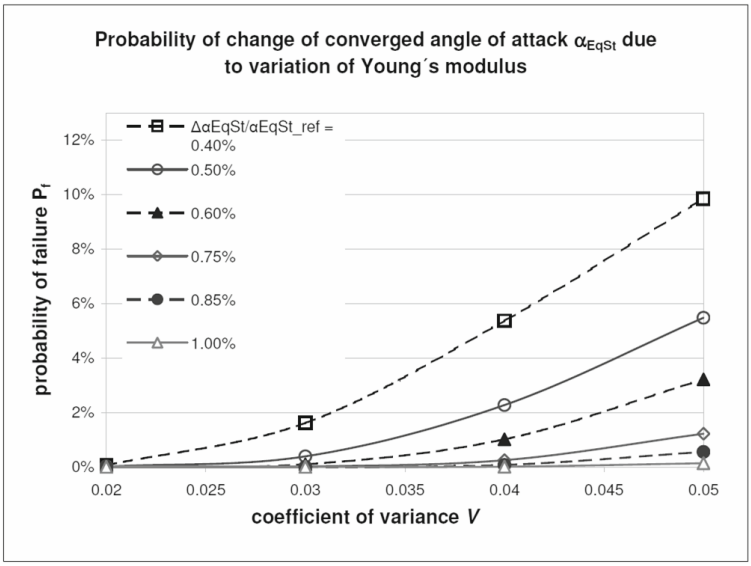

Fig. 10 Probability of deviation of angle of attack caused by variation of Youngt's modulus for different performance criteria

3.6 Conclusions

In the present work, the influence of random structural parameters on the aerodynamic performance of a metallic test wing structure is investigated. The investigations demonstrate the suitability of the FORM analysis to handle some classes of stochastic uncertainties affecting the aeroelastic response of a wing structure. Due to the gradient based optimization procedure, which forms the basis of the FORM the main requirement to the investigated problem is the existence of only one minimum solution for the reliability index β. To handle problems which violate this requirement as there are the uncertainties of fibre orientation angles of composite materials, other stochastic analysis methods like Latin hypercube sampling should be used instead of the FORM.

To reduce the numeric costs of stochastic simulation some simplifications had to be made within the analysis process. The influence of the weight reduction on the target lift caused by reduction of the wall thicknesses was neglected. The simultaneous variation of structural parameters of the top and bottom skin in only four areas represents a highly simplified test case compared to the real structure (cp. the remarks in section 3.4). Considering these simplifications, the results obtained in the present work should represent a conservative trend.

The variation of the input parameters of top and bottom skin parts as well as of spar webs for a higher number of independent areas of variation is a part of actual work as well as the consideration of weight reduction for the target lift. Another effect which could be considered is the tendency of the skin areas to buckle if the

local bending stiffness of the panes is reduced by a variation of structural parameters having a significant influence on the aerodynamic drag.

References

[1] Heinze, W.: Ein Beitrag zur quantitativen Analyse der technischen und wirtschaftlichen Auslegungsgrenzen verschiedener Flugzeugkonzepte für den Transport großer Lasten; ZLR-Forschungsbericht 94-01, Braunschweig (1994)
[2] Österheld, C.M.: Physikalisch begründete Analyseverfahren im integrierten multidisziplinären Flugzeugvorentwurf; ZLR-Forschungsbericht 2003-06, Braunschweig (2003)
[3] Reimer, L., Braun, C., Bae-Hong, C., Ballmann, J.: Computational Aeroelastic Design and Analysis of the HIRENASD Wind Tunnel Wing Model and Tests. In: International Forum on Aeroelasticity and Structural Dynamics (IFASD) 2007, Stockholm, Sweden, Paper IF-077 (2007)
[4] Heinrich, R., Dargel, G.: Spezifikation des Testfalls für den Hauptmeilenstein M8.1 im Verbundvorhaben MEGADESIGN (2006)
[5] Haupt, M., Niesner, R., Unger, R., Horst, P.: Coupling Techniques for Thermal and Mechanical Fluid-Structure-Interactions in Aeronautics. PAMM ů Proc. Appl. Math. Mech. 5, 19–22 (2005)
[6] Schneider, W.: Die Entwicklung und Bewertung von Gewichtsabschätzungsformeln für den Flugzeugvorentwurf unter Zuhilfenahme von Methoden der mathematischen Statistik und Wahrscheinlichkeitsrechnung; Berlin, Techn. Univ., Diss. (1973)
[7] Niu, M.C.Y.: Airframe Structural Design: practical Design Information and Data on Aircraft Structures. Conmilit Pr., Hong Kong (1999)
[8] Patnaik, S., Gendy, A., Berke, L., Hopkins, D.: Modified Fully Utilized Design (MFUD) Method for Stress and Displacement Constraints. NASA Technical Memorandum 4743 (1997)
[9] Malcolm, D.J., Laird, D.L.: Extraction of Equivalent Beam Properties from Blade Models. Wind Energy 10, 135–157 (2007)
[10] Reim, A., Horst, P.: Structural optimization considering stochastic variations of manufacturing alternatives. In: 8th World Congress on Structural and Multidisciplinary Optimization (2009)
[11] Haldar, A., Mahadevan, S.: Probability, Reliability and Statistical Methods in Engineering Design. Wiley & Sons (2000)
[12] Rackwitz, R., Fiessler, B.: Structural Reliability Under Combined load sequences. Computers & Structures 9, 489–494